Application of the Immersed Boundary Method in the Study of Two Tandem Cylinders

Ismar Mascarenhas de Carvalho Filho[1], Caio Lemos Peixoto Martins[1], Mylena Carvalho Silva[1], Andreia Aoyagui Nascimento[12]

[1]*Laboratório de Engenharia Térmica e de Fluidos (LATEF), Escola de Engenharia Elétrica, Mecânica e de Computação (EMC), Universidade Federal de Goiás (UFG)*
Av. Esperança, s/n, Prédio B5, 74690-900, Goiânia, Goiás, Brasil
ismar@discente.ufg.br, caiopeixoto@discente.ufg.br, mylena.carvalho@discente.ufg.br, aanascimento@ufg.br
[2]*Centro de Excelência em Hidrogênio e Tecnologias Energéticas Sustentáveis (CEHTES), Parque Tecnológico Samambaia,*
Rodovia R2, n. 3.061, Campus Samambaia, CEP: 74690-900, Goiânia, Goiás, Brasil
aanascimento@ufg.br

Abstract. The study of fluid flow around various surfaces is crucial in several applications of mechanical engineering, especially in cylindrical geometries of circular section, common in structures such as bridges, wind turbines, cooling systems, and power towers. In this work, we solve the two-dimensional mass conservation and Navier-Stokes equations in the x and y variables, ignoring gravitational effects, applying the Fourier pseudo-spectral method coupled with the immersed boundary method. We define a domain with two cylindrical boundaries of diameter equal to 0.0016m and a low Reynolds number. The obtained results are promising, approaching existing literature reviews.

Keywords: Fourier pseudo-spectral method , Immersed boundary method , Flow over aligned cylinders

1 Introduction

The study of fluid flow around different geometries, especially cylindrical with circular cross-sections, is crucial for various engineering applications such as bridges, wind turbines, cooling systems, and power lines. Computational Fluid Dynamics (CFD) plays an essential role in the development of these projects, enabling the simulation and analysis of fluid behavior under various conditions, including flow patterns, turbulence, heat transfer, and drag coefficient, among other important characteristics. Different computational methods, such as finite volume, finite difference, finite element, and spectral methods, are used to numerically solve the equations describing fluid behavior, each with its specific advantages and limitations depending on the problem and project requirements.

In a numerical investigation, Mloy and Wang [1] studied the effects of spacing on vortex shedding in two cylinders arranged in tandem with Reynolds number $[R_e] = 100$ in a mesh of 512x256. Preliminary tests with flows around one and two cylinders validated the accuracy of the solver used by comparing vortex shedding results and hydrodynamic forces with literature data. The results indicate that the spacing between cylinders can be strategically adjusted to completely suppress vortex shedding in certain configurations, while in others it can partially reduce or not significantly affect this phenomenon.

The work of Tu et al. [2] used two aligned circular section cylinders to validate their finit element method, employing low Reynolds numbers to investigate flow-induced vibrations (VIV) in two elastically mounted circular cylinders arranged in tandem, subjected to a planar shear flow at Re=160.

Another significant study on aligned cylinders is that of Narváez et al. [3], which investigated flow-induced vibrations in two cylinders arranged in tandem under uniform flow with a low Reynolds number. This study validated a code that employs the immersed boundary method, simulating flow with a Reynolds number of 100. The validation was performed by comparing the results with those of Sharman et al. [4] and Mussa et al. [5], using meshes of varying resolutions: 501x361, 751x541, and 1001x721. This approach ensured the accuracy and reliability of the code by confirming the consistency of the results with previous studies.

The present work uses the physical problem of flow over aligned cylinders to validate the in-house, two-dimensional code of the Fourier pseudospectral method coupled to the immersed boundary method, for Re = 100.

2 METHODS

2.1 Physical Problem

Figure (1 (b)) represents the generation of von Kármán vortices. A streamline γ surrounds the vicinity of the cylinder in the boundary layer region. The pressure at point A is higher than at point B (adverse pressure gradient), causing instability in the boundary layer, resulting in its separation near point B. Under these conditions, the adverse pressure gradient is strong enough to reverse the flow direction in the separation region. A von Kármán vortex V is thus created and subsequently transported downstream by the flow. As seen in Fig.(1b)

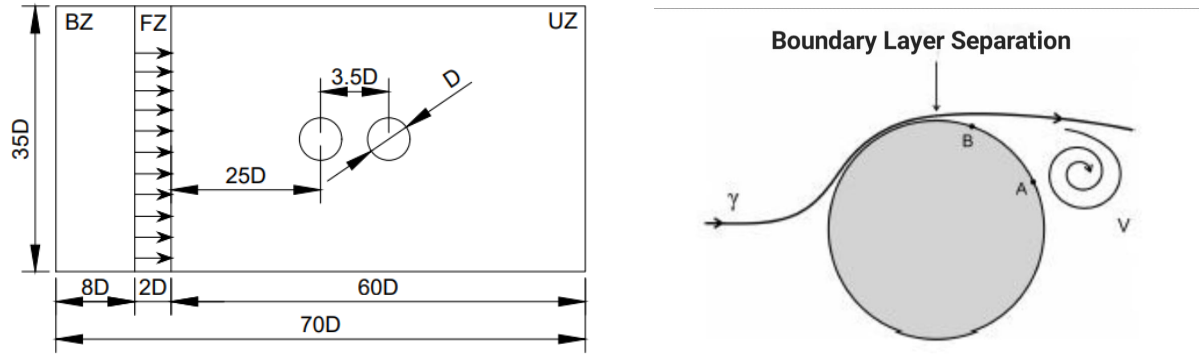

(a) (b)

Figure 1. (a) Diagram of the simulation characteristics, (b) Illustration of Boundary Layer Separation by Marconi and Pereira [6]

Figure (1 (a)) shows the representation of the physical domain, with dimensions of $L_x = 70D$ and $L_y = 35D$ where BZ refers to the buffer zone, FZ refers to the forcing zone, in which a velocity u_{max} is imposed in a rectangular profile to align the flow, and UZ is the useful zone where the flow is analyzed. All dimensions are given dimensionless by the diameters of the cylinders, D. The distance between the first geometry located 25D from FZ and the second at 3.5D of first.

2.2 Mathematical Modeling

The mathematical modeling using the mass conservation equation, eq. (2), and the Navier-Stokes equation, eq. (1). The simplifying assumption used are: incompressible flow, Newtonian fluid, no gravitational effects, and constant properties.

$$\frac{\partial u_j}{\partial t} + \frac{\partial (u_i u_j)}{\partial x_j} = \frac{-\partial P}{\rho \partial x_i} + \nu \left(\frac{\partial^2 u_i}{\partial x_j^2 \partial x_j^2} \right) + \frac{f_i}{\rho} \tag{1}$$

where x and y are the horizontal and vertical directions (of the domain), u and ν are the horizontal and vertical velocities, respectively, μ and ρ are the fluid properties: viscosity and density, and f_x and f_y are the source terms in which the Lagrangian velocities will be inserted.

$$\frac{\partial u}{\partial x} + \frac{\partial v}{\partial y} = 0 \tag{2}$$

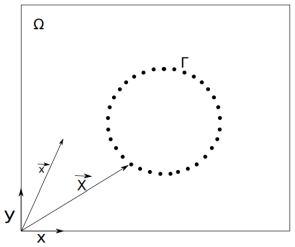

Figure 2. Diagram of the Eulerian and Lagrangian mesh. Nascimento et al. [7]

To model the circular geometry, where the Lagrangian and Eulerian points do not coincide, the force $F_i(x,t)$ is interpolated and distributed over its surroundings. For this purpose, the distribution function $D_h(x-X)$ proposed by Peskin [8] in eq. (3), and the cubic function W_c described by Tornberg A [9] in eq. (4) are used, as stated by Nascimento et al. [10].

$$D_h(\vec{x}-\vec{X}) = \frac{1}{h^2} W_c(r_x) W_c(r_y), \tag{3}$$

$$W_c(r) = \begin{cases} 1 - \frac{1}{2}|r| - |r|^2 + \frac{1}{2}|r|^3 & \text{if } 0 \le |r| \le 1 \\ 1 - \frac{11}{6}|r| + |r|^2 - \frac{1}{6}|r|^3 & \text{if } 1 \le |r| \le 2, \\ 0 & \text{if } 2 \le |r| \end{cases} \tag{4}$$

Where D_h is the distribution function, $r_x = \frac{x-X}{\Delta x}$, $r_y = \frac{y-Y}{\Delta y}$, Δs is the distance of the Lagrangian points, and W_c is the weight function.

2.3 Numerical Modeling

In the present work, an in-house code developed by the mechanical engineering research group at the Federal University of Goiás was utilized to solve the physical problem. The code employs the Fourier pseudo-spectral method, as described by William L. Briggs [11], coupled with the immersed boundary method. The pseudo-spectral method used in this study requires consideration of two domains: physical and spectral. The IMERSEPEC2D methodology developed in Fortran, which applies Fourier transforms to all terms in equations eq. (1) and eq. (2), resulting in the derivation of equations eq. (5) and eq. (6).

$$\imath k_j \hat{u}_j = 0 \tag{5}$$

$$\left[\frac{\partial}{\partial t} + \nu k^2\right] \hat{u}_j(\vec{k},t) = \varphi_{im} \left[\hat{f}_m(\vec{k},t) - \imath k_j \int_{\vec{k}=\vec{r}+\vec{s}} \hat{u}_m(\vec{r},t)\hat{u}_j(\vec{k}-\vec{r},t)d\vec{r}\right] \tag{6}$$

where k is the wave number, Fourier spatial transformation parameter and $\hat{u}_j$ is the transformed velocity vector, $\imath$ is the complex number, and f_i is the source term.

The drag coefficient was obtained from $C_d = \frac{2F_{cx}}{\rho A U_\infty^2}$, where F_{cx} is the total force exerted by the fluid on a body in the x-direction, A is the cross-sectional area interacting with the fluid, and U_∞ is the uniform velocity profile at the inlet.

Simulation Parameters

In current simulation, was used a Reynolds number ($Re = \frac{\rho U_{max} D}{\nu}$) of 100 and a cylinder diameter (D) of 0.0016 m. The simulation domain was discretized using 1024x512 colocation points. The total simulation time was 10 seconds, with a time step (dt) of 10^{-5} seconds. The Courant-Friedrichs-Lewy (CFL) number used was 0.1, and the maximum velocity (U_{max}) achieved was 1 m/s.

3 Results and Discussion

This section will present the results of the numerical validation obtained.

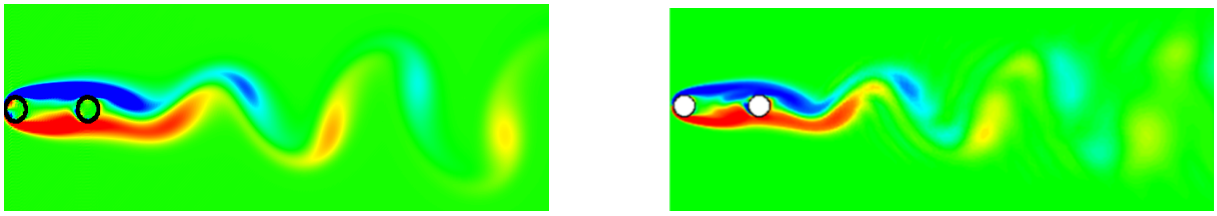

(a) Vorticity (b) Vorticity by Tu et al. [2]

Figure 3. Comparison of Vorticity Visualizations

In Figure (3a), the formation of vortices is observed, with the red color indicating counterclockwise (positive) vortices where the values of $W \leq 4919$, and the blue color representing clockwise (negative) vortices where $W \geq -4893$. These patterns are quite similar to the vorticity shown in Figure (3b), which features 5 vortices and does not show boundary layer separation on the first cylinder, similar to those in Figure (3a). Additionally, the observed vortex shedding in both figures corresponds to the 1S pattern, where a single vortex is shed alternately from each side of the cylinder in each cycle, further highlighting the similarity in the vorticity patterns between the two figures.

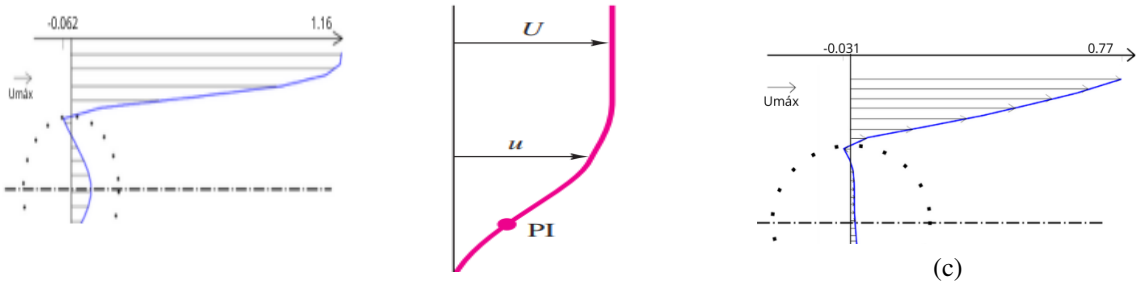

(a) (b) (c)

Figure 4. (a) Velocity profile of upstream cylinder; (b) Velocity profile taken of White [12]; (c) Velocity profile of downstream cylinder.

In Figures (4a) and (4c), it is observed that the profile velocity is zero at the boundary of the geometry, with recirculation occurring inside due to the immersed boundary method, the internal points within the geometry are still influenced by the surrounding flow field due to the way the immersed boundary method handles the geometry. The interpolation of the points in the Lagrangian mesh can lead to residual velocities within the geometry region.

Additionally, Figures (4a) and (4c) show the velocity profiles for the upstream and downstream cylinders, respectively. Both profiles are similar to the one in Figure (4b), which displays a weak adverse pressure gradient.

Authors	Cd_1	Cd_2	Compatibility of Cd_1	Compatibility of Cd_2
Nárvaez et al.	1.17	0.06	99.98%	66.67%
Tu et al.	1.15	0.06	100%	66.67%
Present author	1.15	0.04	-	-

Table 1. Comparative Results with Compatibility

The drag coefficients Cd_1 and Cd_2 correspond to the drag experienced by the first and second cylinder geometries, respectively. The percentage shown under "Compatibility of Cd_1" and "Compatibility of Cd_2" represents how closely the present work's results align with the reference values from the literature.

The obtained values for the drag coefficients were compared with the references in Table (1) below. Cd_1 refers to the drag coefficient for the first cylinder, while Cd_2 corresponds to the drag coefficient for the second cylinder. The "Compatibility" columns show the percentage agreement of the computed drag coefficients with the reference values from Narváez et al. [3] and Tu et al. [2]

4 Conclusions

In this paper, the flow behavior over two aligned cylinders, spaced center-to-center by $3.5D$, was investigated at a Reynolds number of $R_e = 100$. The results indicated that the computed vorticity aligned with existing literature, confirming the accuracy of the numerical data.

Furthermore, the velocity profiles analyzed were consistent with the low Reynolds number employed. Specifically, the observed vortex formation and flow structure correspond with theoretical expectations for this Reynolds number range. This consistency supports the validity of the results and the effectiveness of the applied numerical model.

However, the values of Cd_2 (drag coefficient for the second cylinder) were not satisfactory, and efforts are currently being made to resolve this issue.

Additionally, the study proposes incorporating degrees of freedom in the geometrical configurations to further refine the analysis.

Acknowledgements. The authors thank Eletrobras, the "Programa de Pesquisa e Desenvolvimento Tecnológico" (P&D) of ANEEL, the Foundation for Research Support of the State of Goiás (FAPEG), and the Tutorial Education Program (PET) for the financial support and infrastructure provided for the development of the research.

Authorship statement. The authors hereby confirm that they are the sole liable persons responsible for the authorship of this work, and that all material that has been herein included as part of the present paper is either the property (and authorship) of the authors, or has the permission of the owners to be included here.

References

[1] J. S. Mloy and Y. Wang. Vortex-induced vibrations of two cylinders in tandem arrangement at low reynolds number. *Journal of Fluid Dynamics*, 2023.

[2] J. Tu, D. Zhou, Y. Bao, J. Ma, J. Lu, and Z. Han. Flow-induced vibrations of two circular cylinders in tandem with shear flow at low reynolds number. *Journal of Fluids and Structures*, vol. 59, n. 800, pp. 224–251, 2015.

[3] G. Narváez, E. Schettini, and J. Silvestrini. Numerical simulation of flow-induced vibration of two cylinders elastically mounted in tandem by immersed moving boundary method. *Applied Mathematical Modelling*, 2019.

[4] B. Sharman, F. S. Lien, L. Davidson, and C. Norberg. Numerical predictions of low reynolds number flows over two tandem circular cylinders. *International Journal of Numerical Methods in Fluids*, 2004.

[5] A. Mussa, P. Asinari, and L.-S. Luo. Lattice boltzmann simulations of 2d laminar flows past two tandem cylinders. *Journal of Computational Physics*, 2009.

[6] L. Marconi and R. Pereira. The statistical physics of turbulence. *Revista Brasileira de Ensino de F ´ısica*, 2021.

[7] A. A. Nascimento, F. P. Mariano, and E. L. M. Padilla. Comparison of the convergence rates between fourier pseudospectral and finite volume methods using taylor-green vortex problem. *22nd International Congress of Mechanical Engineering*, 2013.

[8] C. Peskin. Flow patterns around heart valves: a numerical method. *J Comput Phys*, 1972.

[9] E. B. Tornberg A. Numerical approximations of singular source terms in diferential equations. *J Comput Phys*, 2004.

[10] A. A. Nascimento, F. P. Mariano, da A. Silveira Neto, and E. L. M. Padilla. Coupling of the immersed boundary and fourier pseudo-spectral methods applied to solve fuid–structure interaction problems. *Journal of the Brazilian Society of Mechanical Sciences and Engineering*, 2024.

[11] V. E. H. William L. Briggs. *The DFT An Owner's Manual For The Discrete Fourier Transform*. Society for Industrial and Applied Mathematics, 1987.

[12] F. M. White. *Mecânica dos Fluidos*. bookman, 2011.